Superfluid Heat Conduction and the Cooling of Magnetized Neutron Stars

Deborah N. Aguilera,[1] Vincenzo Cirigliano,[2] José A. Pons,[3] Sanjay Reddy,[2] and Rishi Sharma[2]

[1]*Tandar Laboratory, Comisión Nacional de Energía Atómica, Avenida Gral. Paz 1499, 1650 San Martín, Buenos Aires, Argentina*
[2]*Theoretical Division, Los Alamos National Laboratory, Los Alamos, New Mexico 87545, USA*
[3]*Department of Applied Physics, University of Alicante, Apartado de Correos 99, E-03080 Alicante, Spain*

(Received 5 August 2008; revised manuscript received 12 November 2008; published 3 March 2009)

We report on a new mechanism for heat conduction in the neutron star crust. We find that collective modes of superfluid neutron matter, called superfluid phonons, can influence heat conduction in magnetized neutron stars. They can dominate the heat conduction transverse to the magnetic field when the magnetic field $B \gtrsim 10^{13}$ G. At a density of $\rho \simeq 10^{12}$–10^{14} g/cm^3, the conductivity due to superfluid phonons is significantly larger than that due to lattice phonons and is comparable to electron conductivity when the temperature $\simeq 10^8$ K. This new mode of heat conduction can limit the surface anisotropy in highly magnetized neutron stars. Cooling curves of magnetized neutron stars with and without superfluid heat conduction could show observationally discernible differences.

DOI: 10.1103/PhysRevLett.102.091101 PACS numbers: 26.60.Gj, 67.85.De, 97.60.Jd

Multiwavelength observations of thermal emission from the neutron star (NS) surface and explosive events such as superbursts in accreting NSs and giant flares in magnetars provide a real opportunity to probe the NS interior (see [1,2] for recent reviews). Theoretical models of these phenomena underscore the importance of heat transport in the NS crust and have shown that it impacts observations. For example, nearby isolated compact x-ray sources that have also been detected in the optical band have a significant optical excess relative to the extrapolated x-ray blackbody emission (a factor of 5–14) [3]. This optical excess can arise naturally if heat conduction in the NS crust is anisotropic due to the presence of a large magnetic field leading to an anisotropic surface temperature distribution [4–6]. In accreting NSs, conductivity directly affects the observed thermal relaxation time of the crust [7], the superburst ignition, and its recurrence time scale [8].

Typically, heat conduction is due to relativistic electrons. Electrons are numerous and degenerate and provide an efficient mode of heat transport. Conduction due to lattice phonons has been considered and could play a role in the outer crust of highly magnetized neutron stars [5,9]. In this Letter, we demonstrate that a new mechanism for heat transport arising due to the superfluid nature of the inner crust is important at high temperature and/or large magnetic fields. Here the heat is carried by collective excitations of the neutron superfluid called superfluid phonons (SPHs).

This mode of conduction is especially relevant in NSs with moderate to high magnetic fields ($B \gtrsim 10^{13}$ G). Here electron heat transport is anisotropic because electrons move freely only along magnetic field lines. Motion perpendicular to the field is restricted because the electron gyrofrequency is large compared to the inverse collision time. In contrast, SPHs, being electrically neutral excitations, are unaffected by magnetic fields. We find that SPH conduction is typically much larger than the electron conduction transverse to the field and can limit the surface temperature anisotropy in magnetized NSs. At low magnetic fields, SPH conduction can still be relevant when the temperature $T = 10^8$–10^9 K.

Neutrons in the inner crust are expected to form Cooper pairs and become superfluid below the critical temperature $T_c \approx 10^{10}$ K. The superfluid ground state spontaneously breaks baryon-number symmetry and gives rise to a new massless Goldstone mode—the SPH. At long wavelengths, these phonons have a linear dispersion relation $\omega = v_s q$, where $v_s \simeq k_{\rm Fn}/\sqrt{3}M$, M is the mass of the neutron, and $k_{\rm Fn}$ is the neutron Fermi momentum. The thermal conductivity of a weakly interacting gas of SPHs can be computed from kinetic theory and is given by

$$\kappa_{\rm SPH} = \tfrac{1}{3} C_V v_s \lambda_{\rm SPH}, \tag{1}$$

where $C_V = 2\pi^2 T^3/(15 v_s^3)$ is the specific heat of the phonon gas and $\lambda_{\rm SPH}$ is the typical mean free path of a thermal SPH. We can rewrite Eq. (1) using fiducial values of the temperature and the phonon velocity as

$$\kappa_{\rm SPH} = 1.5 \times 10^{22} \left(\frac{T}{10^8\ {\rm K}}\right)^3 \left(\frac{0.1}{v_s}\right)^2 \left(\frac{\lambda_{\rm SPH}}{\rm cm}\right) \frac{\rm erg}{\rm cm\,s\,K}. \tag{2}$$

This is to be compared with the thermal conductivity of electrons in the inner crust which is approximately 10^{18} erg cm^{-1} s^{-1} K^{-1} when $T = 10^8$ K [10]. In what follows, we calculate the SPH mean free path and show that SPH conduction is relevant.

The low-energy degrees of freedom in the inner crust are lattice phonons (LPHs), electrons, and SPHs. At long wavelengths, the excitations of the ion lattice, with mean number density n_I, mass number A, and charge Z, are the longitudinal and transverse LPHs with velocities (in units of c = the speed of light) $c_s = \omega_P/q_{\rm TFe}$ and $c_t \simeq 0.7\omega_P/q_{\rm BZ}$, respectively [11]. Here $\omega_P = \sqrt{4\pi e^2 Z^2 n_I/(AM)}$ is the ion-plasma frequency, $q_{\rm TFe} = \sqrt{4e^2/\pi} p_{\rm Fe}$ is the in-

verse Thomas-Fermi screening length of the electrons, $p_{\rm Fe}$ is the electron Fermi momentum, $q_{\rm BZ} = (4.5\pi)^{1/3} a_i^{-1}$, and $a_i = [3/(4\pi n_I)]^{1/3}$ is the interion distance. The electrons are characterized by their Fermi momentum $p_{\rm Fe} = (3\pi^2 Z n_I)^{1/3} \gg m_e \gg T$ and form a highly degenerate, relativistic Fermi gas. As mentioned earlier, the SPHs are collective excitations of the neutron superfluid, and their interactions are weak at low temperature. Because of the derivative coupling between phonons, the cross section for phonon-phonon scattering is parametrically suppressed by the factor T^8/μ_n^8, where $\mu_n = k_{\rm Fn}^2/2M$ is the neutron chemical potential [12]. We note that when $T \simeq T_c$, SPHs are strongly damped as they can easily decay into neutron particle-hole excitations. However, since the crust cools to $T \ll T_c$ within several hours of the birth of the NS, this process is exponentially suppressed by the factor $\exp(-2T_c/T)$, and the mean free path of SPHs is limited only by their interaction with LPHs, electrons, and impurities.

The relevant processes are illustrated in Fig. 1: (i) Rayleigh scattering of phonons due to interactions with (compositional) impurities in the solid lattice [13]; (ii) absorption of SPHs due to their mixing with the longitudinal lattice phonons which are absorbed efficiently by electrons; and (iii) the decay of a SPH into two LPHs.

At long wavelengths, the cross section for Rayleigh scattering by impurities is

$$\sigma_R = \pi r_0^2 \frac{(q r_0)^4}{1 + (q r_0)^4}, \tag{3}$$

where q is the phonon momentum and r_0 is the strong-interaction length scale related to the neutron-impurity system scattering length. To obtain a conservative estimate of the cross section, we assume that $r_0 \simeq 10$ fm—characteristic of the size of a heavy neutron-rich nucleus. At low temperature, when $q r_0 \ll 1$, the mean free path of SPHs with thermal energy $\omega_{\rm th} = 3T$ is

$$\lambda_{\rm Ray} = (n_{\rm Im}\sigma_R)^{-1} = \frac{v_s^4}{81 n_{\rm Im} \pi r_0^6 T^4}, \tag{4}$$

where $n_{\rm Im} = 3/(4\pi d^3)$ is the impurity number density and d is the interimpurity distance. Using fiducial values we can rewrite Eq. (4) as

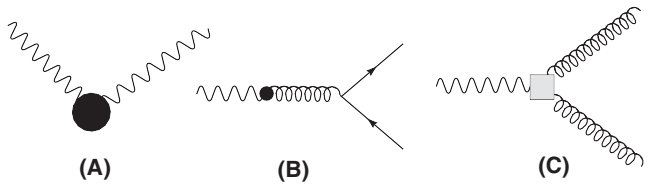

FIG. 1. Phonon scattering processes: (a) Rayleigh scattering; (b) phonon absorption by electrons; and (c) decay of SPHs into lattice phonons. The wavy line is the SPH, the curly line is the LPH, and the solid line is electrons, respectively.

$$\lambda_{\rm Ray} = 450 \left(\frac{v_s}{0.1}\right)^4 \left(\frac{x}{10}\right)^3 \left(\frac{10\ {\rm fm}}{r_0}\right)^3 T_7^{-4}\ {\rm cm}, \tag{5}$$

where $x = d/r_0$ is the diluteness parameter for the impurities and T_7 is the temperature in 10^7 K.

We now show that inelastic processes such as SPH absorption by electrons and decay to LPHs shown in Figs. 1(b) and 1(c) are more relevant. To study these processes, we need a low-energy effective theory which couples SPHs and LPHs. On general grounds, this effective theory can contain only derivative terms, and at low temperature it is sufficient to retain the leading terms. The leading order Lagrangian that describes these interactions is of the form

$$\mathcal{L}_{\rm eff} = g_{\rm mix} \partial_0 \phi \partial_i \xi^i + \frac{g_{\rm mix}}{\Lambda^2} \partial_0 \phi \partial_i \xi_i \partial_i \xi_i + \frac{g_{\rm mix}}{\Lambda_t^2} \partial_0 \phi \partial_i \xi_j \partial_i \xi_j + \cdots, \tag{6}$$

where ϕ and $\xi_{i=1\ldots3}$ are the SPH and LPH (canonically normalized) fields, respectively. The first term describes the mixing between longitudinal LPHs and SPHs, and the second and third terms describe the process for the decay of a SPH into two longitudinal or transverse LPHs, respectively.

The coefficients of this effective theory are determined by first calculating the coupling between neutrons and lattice phonons [14]. Here we provide a heuristic derivation, and a detailed derivation will be described in Ref. [15]. We begin with the fundamental short-range interaction between neutrons and ions given by

$$\mathcal{H}_{\rm nI} = \int d^3x d^3x' \Psi_I^\dagger(x) \Psi_I(x) V(x - x') \psi_n^\dagger(x) \psi_n(x),$$

where $V(x - x')$ is the neutron-ion low-energy potential. The neutron-ion interaction is determined by the neutron-ion scattering length $a_{\rm nI}$ and the effective range $r_{\rm nI}$. Both of these quantities are not known for the very neutron-rich nuclei in the inner crust, but $|a_{\rm nI}| \simeq 10$ fm and $r_{\rm nI} = 2$ fm in large stable nuclei. We will use these as fiducial values in our study. When $k_{\rm Fn} a_{\rm nI} \lesssim 1$, the neutron-ion potential is $V(x - x') = 2\pi a_{\rm nI} \delta^3(x - x')/M$. By expanding the ion and neutron density fluctuations in terms of their collective modes, we obtain

$$g_{\rm mix} = 2 a_{\rm nI} \sqrt{\frac{n_I k_{\rm F_n}}{AM^2}}, \qquad \Lambda^2 = \sqrt{n_I A M}, \tag{7}$$

respectively. With increasing density, Pauli blocking of intermediate neutron states modifies the neutron-ion interaction. This effect becomes important when $k_{\rm Fn} a_{\rm nI} \gtrsim 1$ and can be incorporated by replacing the free-space neutron-ion potential by the in-medium T matrix [14]. This is equivalent to replacing $a_{\rm nI}$ in Eq. (7) by $\tilde{a}_{\rm nI} = a_{\rm nI}/(1 + A k_{\rm Fn} a_{\rm nI})$, where the constant $A \simeq 0.4$ is fairly insensitive to the superfluid gap. When $k_{\rm Fn} r_{\rm nI} \gtrsim 1$, we

find that $\tilde{a}_{\rm nI} = a_{\rm nI}/(1 + Ak_{\rm Fn}a_{\rm nI} + Br_{\rm nI}a_{\rm nI}k_{\rm Fn}^2)$, where $B \simeq 0.5$. Interestingly, when $k_{\rm Fn}a_{\rm nI} \gg 1$, the neutron-ion interaction is suppressed and independent of the large vacuum scattering length.

Mixing between SPHs and LPHs will damp SPH propagation because LPHs are strongly damped due to their interaction with electrons. To leading order in the small mixing parameter $g_{\rm mix}$, the mean free path of SPHs with energy ω is given by

$$\lambda_{\rm abs}(\omega) = \frac{v_s^2}{g_{\rm mix}^2} \frac{1 + (1-\alpha^2)^2(\omega\tau_{\rm LPH})^2}{\alpha(\omega\tau_{\rm LPH})^2} \lambda_{\rm LPH}(\omega), \quad (8)$$

where $\alpha = c_s/v_s$ and $\lambda_{\rm LPH}$ and $\tau_{\rm LPH} = \lambda_{\rm LPH}/c_s$ are the mean free path and lifetime of the LPH, respectively. At low temperature, where umklapp processes are frozen, we can estimate $\lambda_{\rm LPH}$ by assuming that LPHs decay primarily by producing particle-hole excitations (normal processes) in the degenerate electron gas. We find that

$$\lambda_{\rm LPH-N}(\omega) = f_{\rm ep}^2 \frac{2\pi c_s^2}{p_{\rm Fe}^2\omega} = \frac{2}{3\pi c_s^2} \frac{Z}{A} \frac{p_{\rm Fe}}{M\omega} = \frac{2}{\pi\omega}, \quad (9)$$

where $f_{\rm ep} = Z\sqrt{n_I/AM}/c_s^2$ is related to the electron-phonon coupling constant [16].

When $T \gtrsim T_{\rm Um} = Z^{1/3}e^2\omega_P/3$, the umklapp processes begin to dominate [17], and in this regime $\lambda_{\rm LPH-U} \simeq 100a_i \simeq 2000$ fm [9]. The corresponding SPH mean free path is in the range 10^{-1}–10^{-4} cm. At intermediate temperatures, we employ a simple interpolation formula given by

$$\lambda_{\rm LPH}^{-1} = f_u\lambda_{\rm LPH-U}^{-1} + (1-f_u)\lambda_{\rm LPH-N}^{-1}, \quad (10)$$

where $f_u = \exp(-T_{\rm Um}/T)$ [17].

Finally, we analyze the decay process shown in Fig. 1(c) described by the second term in Eq. (6). When $v_s \geq c_s$, this decay is kinematically allowed. The amplitude for the SPH of frequency ω to split into two longitudinal LPHs of momentum q_1 and q_2 is given by

$$\mathcal{A} \simeq \frac{g_{\rm mix}}{\Lambda^2}\omega q_1 q_2. \quad (11)$$

The corresponding mean free path for a thermal phonon with energy $\omega = 3T$ can be calculated, and we find that

$$\lambda_{\rm decay} \simeq \frac{863}{f(\alpha)} \left(\frac{10^{-6}}{g_{\rm mix}^2}\right) \left(\frac{c_s}{0.01}\right)^7 \left(\frac{v_s}{0.1}\right) \Lambda_0^4 T_7^{-5} \text{ cm}, \quad (12)$$

where $\Lambda_0 = \Lambda/50$ MeV and $f(\alpha) = 1 - 2\alpha^2/3 + \alpha^4/5$. For the temperatures of relevance we find that $\lambda_{\rm abs} \ll \lambda_{\rm decay}$ and $\lambda_{\rm abs} \ll \lambda_{\rm Ray}$. Consequently, only the SPH absorption process with the mean free path given by Eq. (8) is relevant.

In Fig. 2, we employ the above result [Eq. (8)] for the SPH mean free path and compare the thermal conductivity due to electron, LPH, and SPH transport in a typical NS crust, at temperatures of 10^8 and 10^7 K. We show the

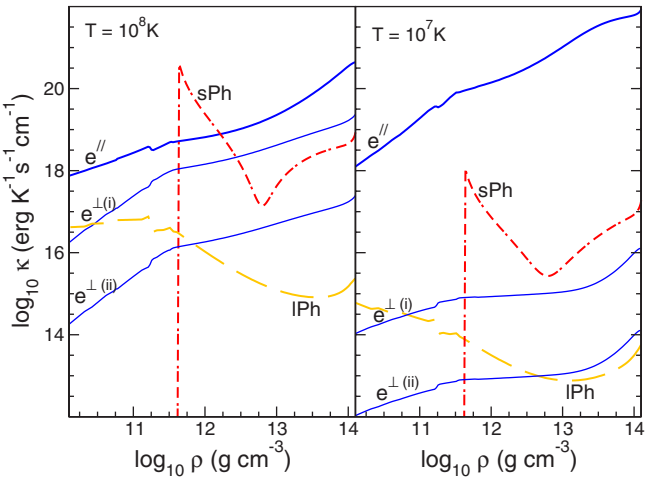

FIG. 2 (color online). Thermal conductivity in a NS crust for $T = 10^8$ K (left) and $T = 10^7$ K (right). The dotted-dashed (red) curve shows the contribution due to SPHs. The thick (thin) solid lines show the electron conductivity in the direction longitudinal (perpendicular) to the magnetic field lines for $B = 10^{13}$ G (i) and $B = 10^{14}$ G (ii). The dashed line (yellow) is the LPH contribution.

electron contribution parallel ($e^{\parallel}$) and perpendicular ($e^{\perp}$) to the magnetic field lines for $B = 10^{13}$ G and $B = 10^{14}$ G, according to [18]. In the outer crust, heat conduction transverse to the field is dominated by LPHs [9]. Here transverse LPHs dominate due to their larger number density, and we use the results from [9]. Above the neutron drip, we find that heat conduction due to SPH (red dotted-dashed curve) is relevant and is always more efficient than conduction due to LPHs. SPH conductivity decreases with depth and reaches a minimum at $v_s = c_s$ due to resonant mixing. Near the neutron drip, where $v_s \ll c_s$, SPHs even dominate over electron conductivity along the field. In the direction transverse to the magnetic field, the SPH conduction is shown to be relevant over much of the inner crust for fields $B > 10^{14}$ G.

To assess how this new mode of conduction might affect observable aspects, we have performed magnetar cooling simulations with and without including SPH conduction. Details regarding the simulation and the input physics are described in earlier work [19]. The new ingredients here are the SPH contribution to the thermal conductivity and the use of an updated $^1S_0$ neutron superfluid gap obtained from quantum Monte Carlo simulations [20]. The cooling curves and temperature profiles for a NS model (model A from Ref. [19]) with a poloidal, crustal magnetic field of strength $B = 5 \times 10^{13}$ G at the magnetic pole are shown in Fig. 3. The temperature at the magnetic equator is shown as long-dashed lines for the model without SPHs and as dashed-dotted lines for the model with SPHs. The temperature at the pole is shown as solid lines for the model without SPHs and as short-dashed lines for the model with SPHs. The left panels show the temperature at the neutron-

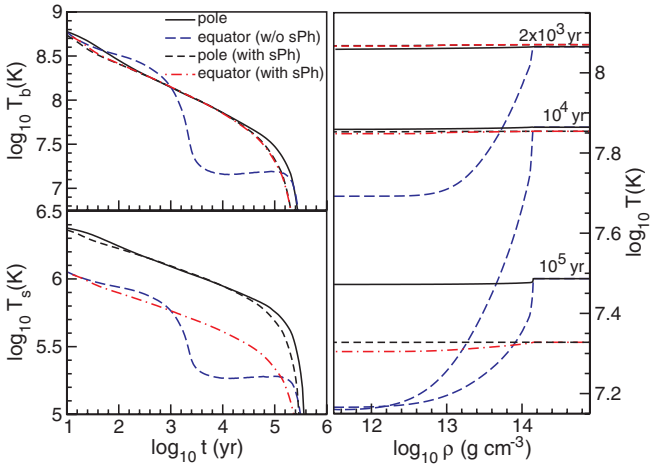

FIG. 3 (color online). Cooling curves of magnetized NS with and without SPH conduction. Left panel: Temperature at the neutron drip (T_b) and at the surface (T_S) vs age. Right panel: T vs density along the polar (solid line) and equatorial directions. The temperature at the equator with SPHs (dashed-dotted line) and without SPHs (dashed line) differ significantly.

drip point denoted by T_b ($\rho \approx 3 \times 10^{11}$ g cm^{-3}) and surface temperature denoted by T_S as a function of the NS age t. From the top panel, we see that the SPH conduction is able to completely erase the temperature anisotropy in the inner crust. The surface temperature anisotropy is suppressed especially for $t \gtrsim 10^3$ yrs and is solely due to anisotropic electron conduction in the outer crust. In the right panel, we show the temperature profile in the inner NS crust along and transverse to the magnetic field at $t = 2 \times 10^3$, 10^4, and 10^5 yrs. SPH conduction is large enough to flatten the huge temperature gradient in the inner crust transverse to the field.

Our estimate for the SPH conductivity, based on Eq. (1), can be improved by replacing the typical mean free path by an appropriate thermal average and by accounting for composition and nuclear structure dependence of the neutron-nucleus scattering potential for neutron-rich nuclei in the crust. We also remark that phonon conductivity can be anisotropic because magnetic fields will induce an anisotropy in the phonon-electron absorption rate. When the spacing between Landau levels becomes comparable to the temperature, phonons propagating transverse to the magnetic field cannot excite single electron-hole states, and this is likely to enhance both LPH and SPH conductivity transverse to the field. These issues warrant further investigation. Nonetheless, our present study clearly demonstrates that SPHs are important for heat conduction and are primarily damped through their mixing with longitudinal lattice phonons. The SPH contribution is significantly larger than LPHs, and the temperature anisotropy in the inner crust is removed by superfluid heat conduction. If future observations allow us to establish a clear correlation among surface temperature distribution, magnetic field orientation, and age, we may be able to probe the superfluid nature of the NS inner crust.

We thank the participants of the INT workshop on the neutron star crust, especially C. Horowitz and A. Cumming, for stimulating discussions. We also thank T. Bhattacharya, A. Chugunov, J. A. Miralles, and D. Yakovlev for discussions and correspondence. This research was supported by the Department of Energy under Contract No. DE-AC52-06NA25396, by the Spanish MEC Grant No. AYA 2004-08067-C03-02, and by CONICET, Argentina. The work of S. R. was funded in part by the LDRD program at LANL under Grant No. 20080130DR.

[1] D. G. Yakovlev and C. J. Pethick, Annu. Rev. Astron. Astrophys. **42**, 169 (2004).
[2] D. Page and S. Reddy, Annu. Rev. Nucl. Part. Sci. **56**, 327 (2006).
[3] F. Haberl, Astrophys. Space Sci. **308**, 181 (2007).
[4] U. Geppert, M. Küker, and D. Page, Astron. Astrophys. **426**, 267 (2004).
[5] J. F. Perez-Azorin, J. A. Miralles, and J. A. Pons, Astron. Astrophys. **451**, 1009 (2006).
[6] U. Geppert, M. Küker, and D. Page, Astron. Astrophys. **457**, 937 (2006).
[7] P. S. Shternin, D. G. Yakovlev, P. Haensel, and A. Y. Potekhin, Mon. Not. R. Astron. Soc. **382**, L43 (2007).
[8] E. F. Brown, L. Bildsten, and R. E. Rutledge, Astrophys. J. **504**, L95 (1998).
[9] A. I. Chugunov and P. Haensel, Mon. Not. R. Astron. Soc. **381**, 1143 (2007).
[10] P. S. Shternin and D. G. Yakovlev, Phys. Rev. D **74**, 043004 (2006).
[11] E. Flowers and N. Itoh, Astrophys. J. **206**, 218 (1976).
[12] D. T. Son and M. Wingate, Ann. Phys. (N.Y.) **321**, 197 (2006).
[13] G. Baym and C. Ebner, Phys. Rev. **164**, 235 (1967).
[14] A. Fetter and J. Walecka, *Quantum Theory of Many-Particle Systems* (McGraw-Hill, New York, 1971), Vol. 26.
[15] V. Cirigliano, S. Reddy, and R. Sharma (to be published).
[16] J. M. Ziman, *Electrons and Phonons* (Oxford University Press, Oxford, 1960).
[17] O. Y. Gnedin, D. G. Yakovlev, and A. Y. Potekhin, Mon. Not. R. Astron. Soc. **324**, 725 (2001).
[18] A. Y. Potekhin, Astron. Astrophys. **351**, 787 (1999).
[19] D. N. Aguilera, J. A. Pons, and J. A. Miralles, Astron. Astrophys. **486**, 255 (2008).
[20] A. Gezerlis and J. Carlson, Phys. Rev. C **77**, 032801 (2008).